Vortex-induced vibrations (VIV)

PEF 6000 - Special topics on dynamics of structures

Associate Professor Guilherme R. Franzini

- To present the physical aspects of the VIV phenomenon. Focus on the flow around a cylinder and the vortex-shedding phenomenon!

- To present the physical aspects of the VIV phenomenon. Focus on the flow around a cylinder and the vortex-shedding phenomenon!
- Examples of references: Textbooks by Blevins (2001), Païdoussis et al (2011), Naudascher & Rockwell (2005), the reviews by Sarpkaya (2004) and Williamson & Govardhan (2004) e selected papers.

- To present the physical aspects of the VIV phenomenon. Focus on the flow around a cylinder and the vortex-shedding phenomenon!
- Examples of references: Textbooks by Blevins (2001), Païdoussis et al (2011), Naudascher & Rockwell (2005), the reviews by Sarpkaya (2004) and Williamson & Govardhan (2004) e selected papers.
- The graduate course PNV5203 - Fluid-Structure Interaction 1 brings deeplier concepts on the theme.

- A cylinder immersed in fluid can oscillate either by the action of prescribed motions (forced oscillations) or due to the fluid-structure interaction. The lattes condition is focus of this class.
- The oscillations leads to modification in the flow field. Among the modifications, we highlight
  1. Increase in the vortex strength;

- A cylinder immersed in fluid can oscillate either by the action of prescribed motions (forced oscillations) or due to the fluid-structure interaction. The lattes condition is focus of this class.
- The oscillations leads to modification in the flow field. Among the modifications, we highlight
  1. Increase in the vortex strength;
  2. Increase in the correlation length;

- A cylinder immersed in fluid can oscillate either by the action of prescribed motions (forced oscillations) or due to the fluid-structure interaction. The lattes condition is focus of this class.
- The oscillations leads to modification in the flow field. Among the modifications, we highlight
  1. Increase in the vortex strength;
  2. Increase in the correlation length;
  3. Increase in the mean drag coefficient;

- A cylinder immersed in fluid can oscillate either by the action of prescribed motions (forced oscillations) or due to the fluid-structure interaction. The lattes condition is focus of this class.
- The oscillations leads to modification in the flow field. Among the modifications, we highlight
  1. Increase in the vortex strength;
  2. Increase in the correlation length;
  3. Increase in the mean drag coefficient;
  4. Changes in the vortex-shedding pattern.

Self-excited and self-limited resonant phenomenon;

Self-excited and self-limited resonant phenomenon;

- VIV of rigid cylinders, mounted on elastic supports that allow oscillations only in the cross-wise direction (VIV-1dof);

Self-excited and self-limited resonant phenomenon;

- VIV of rigid cylinders, mounted on elastic supports that allow oscillations only in the cross-wise direction (VIV-1dof);
- VIV of rigid cylinders, mounted on elastic supports that allow oscillations in the cross-wise direction and in the in-line directions(VIV-2dof);

Self-excited and self-limited resonant phenomenon;

- VIV of rigid cylinders, mounted on elastic supports that allow oscillations only in the cross-wise direction (VIV-1dof);
- VIV of rigid cylinders, mounted on elastic supports that allow oscillations in the cross-wise direction and in the in-line directions(VIV-2dof);
- VIV of flexible cylinders.

Description

- Rigid cylinder of immersed length L, assembled onto an elastic support of stiffness k and damping constant c. The total oscillating mass is m and oscillations are allowed only in the cross-wise direction. The free-stream velocity is uniform and time-invariant of value U_∞.

Setup

Free-stream velocity align with the x direction

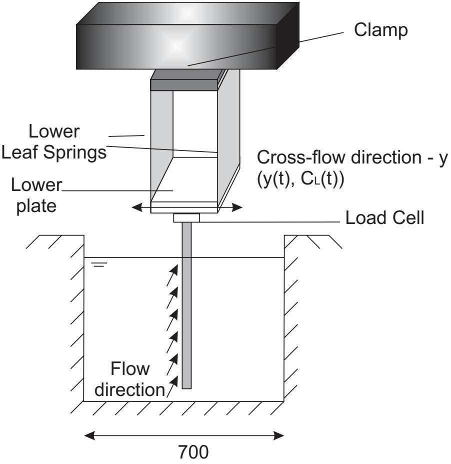

Extracted from Franzini et al (2012).

Tabela: Important quantities. Adapted from Khalak & Williamson (1999).

Quantity	Symbol	Definition
Mass ratio parameter	m^*	$\frac{m_s}{\rho \pi D^2 L/4}$
Structural damping ratio	ζ	$\frac{c_s}{2\sqrt{k(m_s+ma^{pot})}}$
Natural frequency in still water	f_N	$\sqrt{\frac{k}{m+ma^{pot}}}$
Reduced velocity	V_R	$\frac{U_\infty}{f_N D}$
Dimensionless amplitude	A^*	$\frac{A_y}{D}$
Dimensionless frequency	f^*	$\frac{f}{f_N}$
Drag coefficient	C_D	$\frac{F_D}{\frac{1}{2}\rho U_\infty^2 DL}$
Lift coefficient	C_L	$\frac{F_L}{\frac{1}{2}\rho U_\infty^2 DL}$
Reynolds number	Re	$\frac{U_\infty D}{\nu}$

- Term of the hydrodynamic load in phase with the cylinder acceleration. It is also associated with the fluid's kinetic energy;

- Term of the hydrodynamic load in phase with the cylinder acceleration. It is also associated with the fluid's kinetic energy;
- Within potential flow theory, it is the force that the fluid imposed on an oscillating body $F = -m_a \ddot{u}$;

- Term of the hydrodynamic load in phase with the cylinder acceleration. It is also associated with the fluid's kinetic energy;
- Within potential flow theory, it is the force that the fluid imposed on an oscillating body $F = -m_a\ddot{u}$;
- Also in the context of the potential flow theory, a circular cylinder immersed in an infinity domain has its added mass coefficient $C_a = m_a/m_d = 1$, m_d being the mass of fluid displaced by the body;

- Term of the hydrodynamic load in phase with the cylinder acceleration. It is also associated with the fluid's kinetic energy;
- Within potential flow theory, it is the force that the fluid imposed on an oscillating body $F = -m_a \ddot{u}$;
- Also in the context of the potential flow theory, a circular cylinder immersed in an infinity domain has its added mass coefficient $C_a = m_a/m_d = 1$, m_d being the mass of fluid displaced by the body;
- Considering viscous fluids, the added mass coefficient may be significantly different from 1.

- In the flow around a fixes cylinder, the lift force can be assumed as harmonic and monochromatic as $F_L(t) = \hat{F}_L \sin \omega_s t, \quad \omega_s = 2\pi f_s = 2\pi \frac{StU_\infty}{D}$, ω_s being the vortex-shedding frequency;

- In the flow around a fixes cylinder, the lift force can be assumed as harmonic and monochromatic as $F_L(t) = \hat{F}_L \sin \omega_s t, \quad \omega_s = 2\pi f_s = 2\pi \frac{StU_\infty}{D}$, ω_s being the vortex-shedding frequency;
- If the rigid cylinder is assembled onto an elastic support, the natural frequency of the system is $f_N = \frac{1}{2\pi}\sqrt{\frac{k}{m+m_a^{pot}}}$.

- In the flow around a fixes cylinder, the lift force can be assumed as harmonic and monochromatic as $F_L(t) = \hat{F}_L \sin \omega_s t, \quad \omega_s = 2\pi f_s = 2\pi \frac{StU_\infty}{D}$, ω_s being the vortex-shedding frequency;
- If the rigid cylinder is assembled onto an elastic support, the natural frequency of the system is $f_N = \frac{1}{2\pi}\sqrt{\frac{k}{m+m_a^{pot}}}$.
- If $f_s \approx f_N \rightarrow$ Resonance.

- In the flow around a fixes cylinder, the lift force can be assumed as harmonic and monochromatic as $F_L(t) = \hat{F}_L \sin \omega_s t, \quad \omega_s = 2\pi f_s = 2\pi \frac{StU_\infty}{D}$, ω_s being the vortex-shedding frequency;
- If the rigid cylinder is assembled onto an elastic support, the natural frequency of the system is $f_N = \frac{1}{2\pi}\sqrt{\frac{k}{m+m_a^{pot}}}$.
- If $f_s \approx f_N \rightarrow$ Resonance.
- Lock-in: $3 < V_R < 12$ ans is characterized by $f_s \approx f_N \rightarrow$. As the cylinder oscillates, the wake is modified and, consequently, the Strouhal number changes.

- In the flow around a fixes cylinder, the lift force can be assumed as harmonic and monochromatic as $F_L(t) = \hat{F}_L \sin \omega_s t, \quad \omega_s = 2\pi f_s = 2\pi \frac{StU_\infty}{D}$, ω_s being the vortex-shedding frequency;
- If the rigid cylinder is assembled onto an elastic support, the natural frequency of the system is $f_N = \frac{1}{2\pi}\sqrt{\frac{k}{m+m_a^{pot}}}$.
- If $f_s \approx f_N \rightarrow$ Resonance.
- Lock-in: $3 < V_R < 12$ ans is characterized by $f_s \approx f_N \rightarrow$. As the cylinder oscillates, the wake is modified and, consequently, the Strouhal number changes.
- Under *lock-in*, the cylinder oscillates due to the flow excitation, giving rise to the vortex-induced vibration (VIV) phenomenon. The maximum oscillation amplitude is close to one diameter.

Experiments carried out using water as the surrounding fluid have smaller values of m^* than those developed in air

Franzini et al (2012): Experiments in water, $m^* = 2.6$; $m^*\zeta = 0.0018$

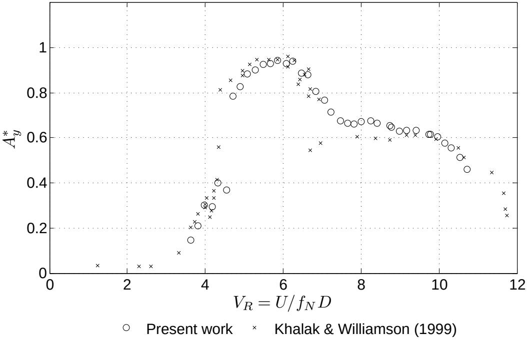

Extracted from Franzini et al. (2012).

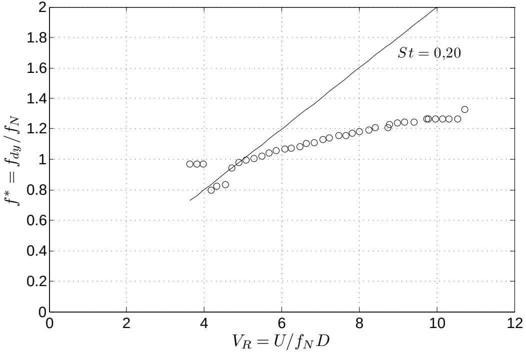

Extracted from Franzini et al. (2012).

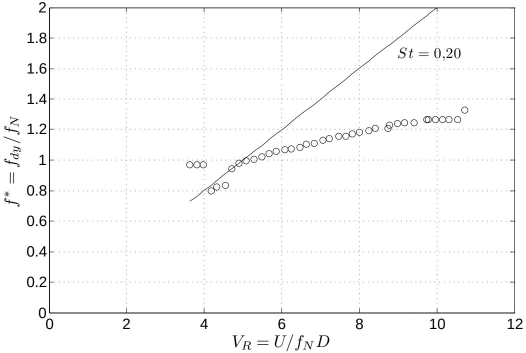

Extracted from Franzini et al. (2012).

- The dimensionless oscillation frequency does not remain constant and close to 1 for systems with low value of $m^*\zeta$.

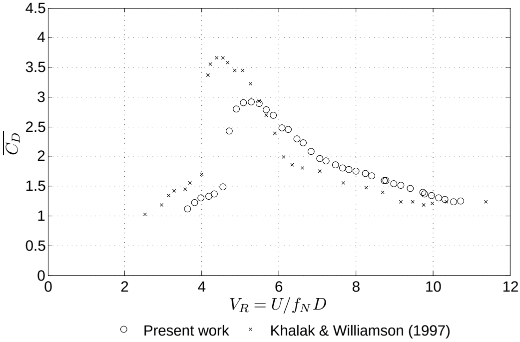

Extracted from Franzini et al. (2012).

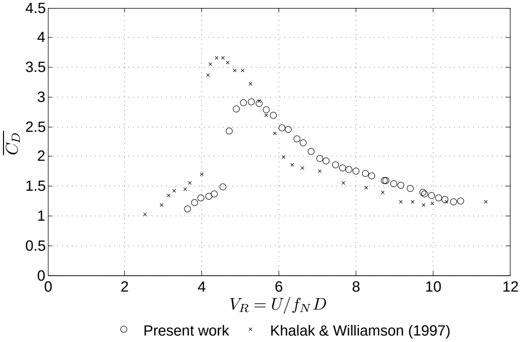

Extracted from Franzini et al. (2012).

- Marked amplification of the mean drag coefficient within the lock-in.

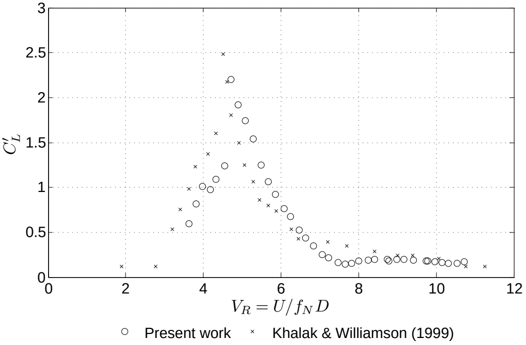

Extracted from Franzini et al. (2012).

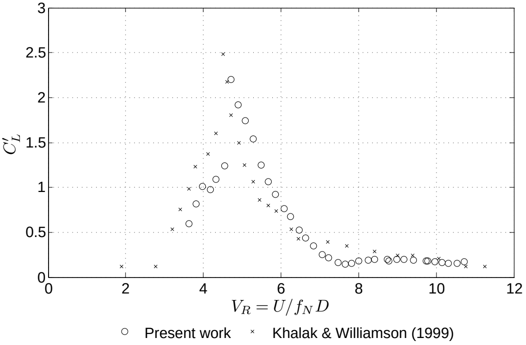

Extracted from Franzini et al. (2012).

- Marked amplification of the rms lift coefficient within the lock-in.

Experiments carried out by Feng (1968): $m^* = 248$

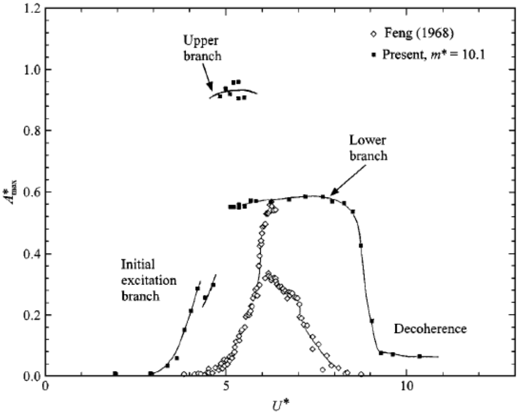

Extracted from Khalak & Williamson (1999).

Depending on the response branch, the vortex-shedding pattern can be modified
2S pattern: Two vortexes are shed at each cycle of cylinder oscillation.

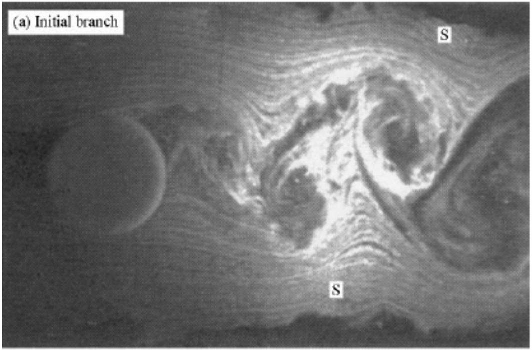

Extracted from Khalak & Williamson (1999).

2P Pattern: Two pairs of vortexes are shed at each cycle of cylinder oscillation.

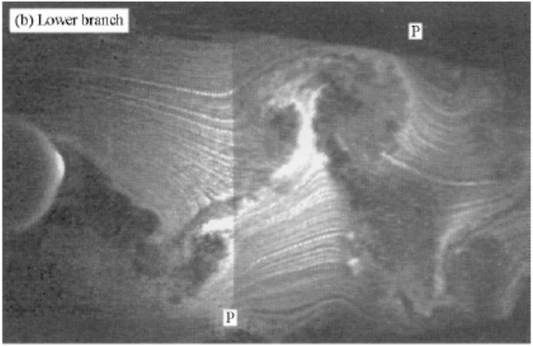

Extracted from Khalak & Williamson (1999).

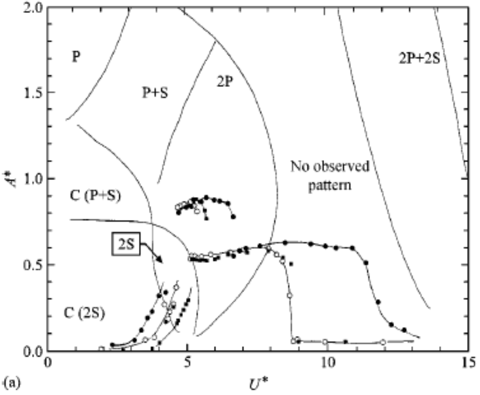

Extracted from Khalak & Williamson (1999).

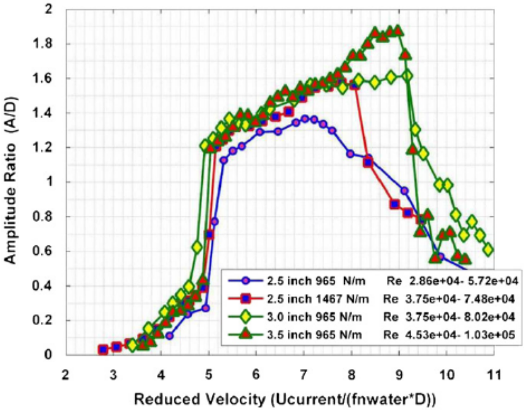

Extracted from Raghavan & Bernitsas (2011).

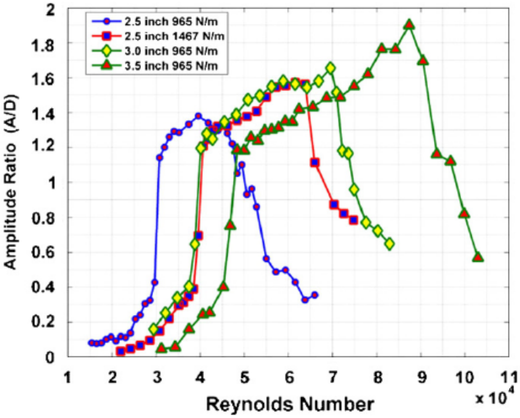

Extracted from Raghavan & Bernitsas (2011).

Programa de Pós-Graduação em Engenharia Civil
Escola Politécnica da Universidade de São Paulo

Focus of the class $f_{N,x} = f_{N,y}$

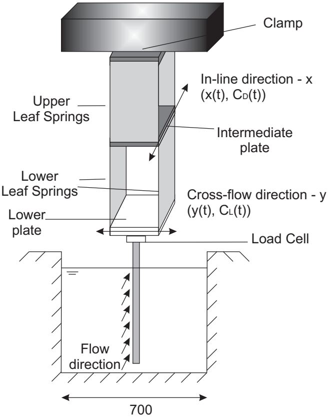

Extracted from Franzini et al (2012).

Characteristic curves, $m^* = 2.6, \zeta = 0.0018$.

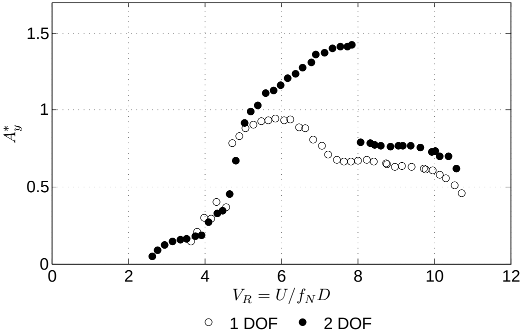

Extracted from Franzini et al (2012).

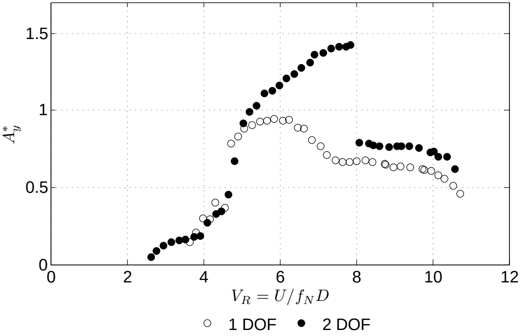

- The presence of in-line oscillations increases the cross-wise oscillations;

Extracted from Franzini et al (2012).

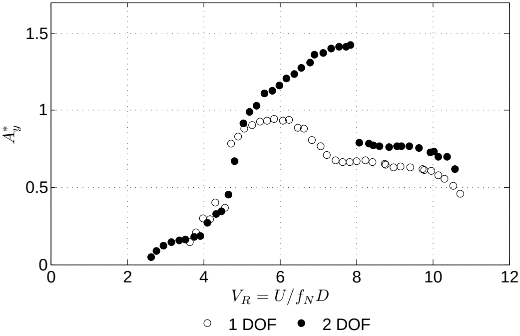

- The presence of in-line oscillations increases the cross-wise oscillations;
- Maximum oscillation amplitudes occurs at $V_R \approx 8$.

Extracted from Franzini et al (2012).

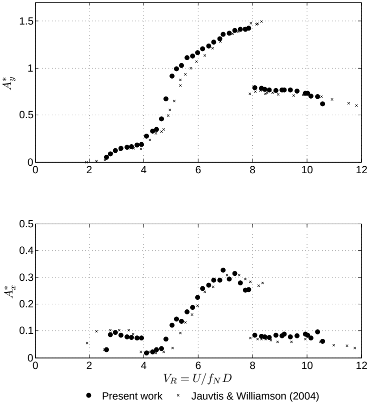

Extracted from Franzini et al (2012).

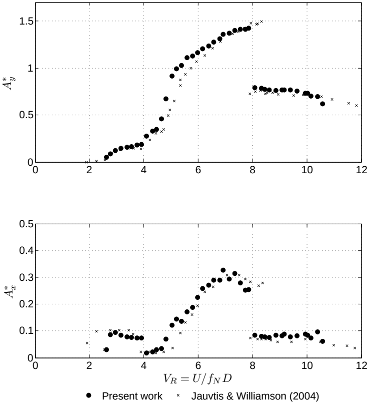

- In-line responses are smaller than those observed in the cross-wise oscillations

Extracted from Franzini et al (2012).

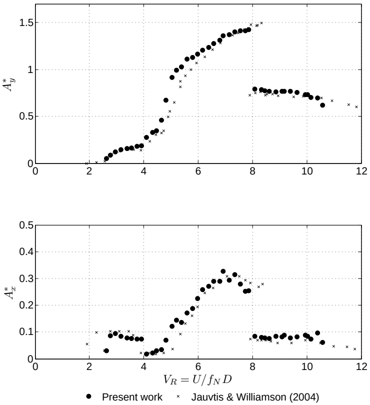

Extracted from Franzini et al (2012).

- In-line responses are smaller than those observed in the cross-wise oscillations
- In-line resonance: $2 < V_R < 4$.

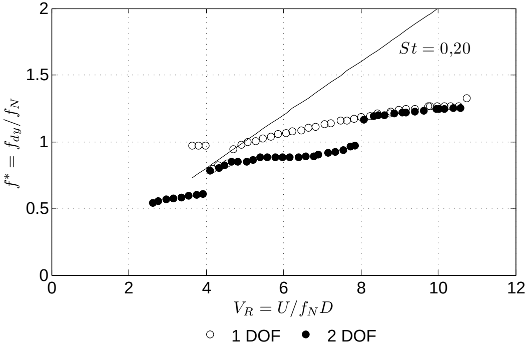

Extracted from Franzini et al (2012).

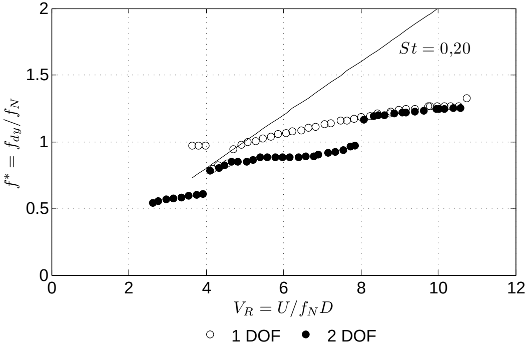

Extracted from Franzini et al (2012).

- Oscillation frequency does not remain constant and close to 1 for systems with low $m^*\zeta$.

Characteristic curves, $m^* = 2.6, \zeta = 0.0018$.

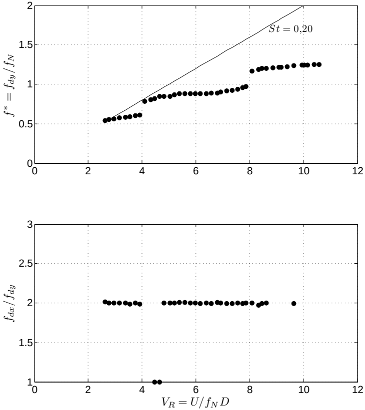

Extracted from Franzini et al (2012).

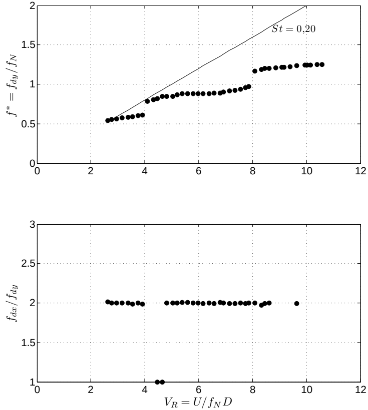

Extracted from Franzini et al (2012).

- In-line oscillations: $f_{d,x} = 2f_{d,y}$.

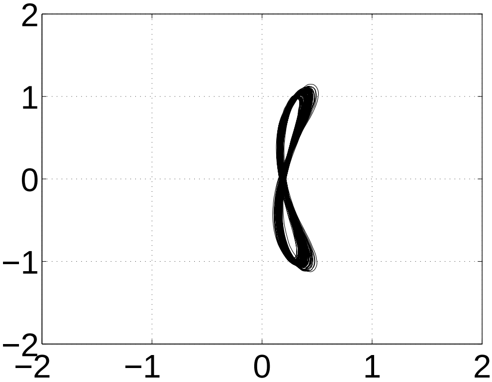

Extracted from Franzini et al (2012).

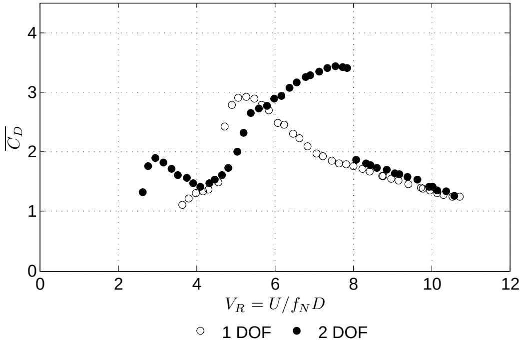

Extracted from Franzini et al (2012).

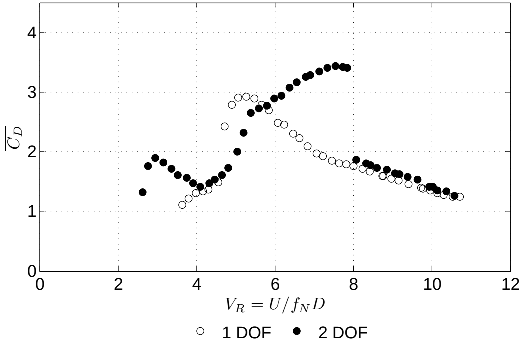

Extracted from Franzini et al (2012).

- The amplification in the mean drag coefficient follows the increase in the oscillation amplitude.

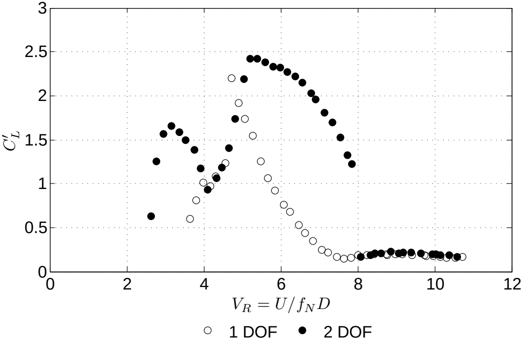

Extracted from Franzini et al (2012).

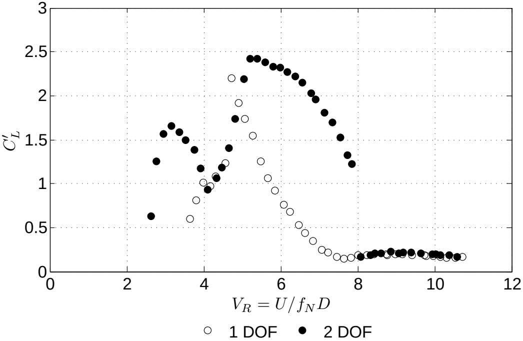

Extracted from Franzini et al (2012).

- Amplification in the r.m.s of the lift coefficient whitin the lock-in.

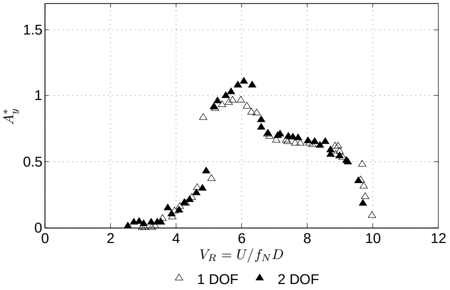

Extracted from Franzini et al (2012).

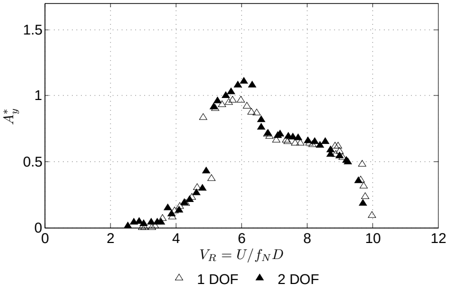

Extracted from Franzini et al (2012)

- Despite free to oscillate in the horizontal plane, oscillation amplitudes in the in-line direction are negligible and the characteristic oscillation amplitudes associated with the cross-wise direction agree with the result obtained for VIV-1dof;

Characteristic curves, $m^* = 8.1, \zeta = 0.0018$.

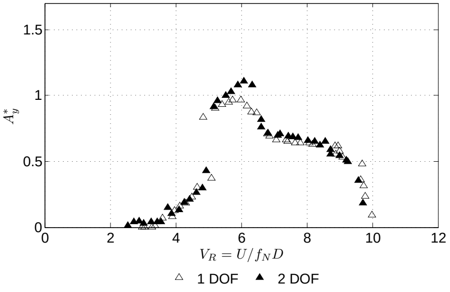

Extracted from Franzini et al (2012)

- Despite free to oscillate in the horizontal plane, oscillation amplitudes in the in-line direction are negligible and the characteristic oscillation amplitudes associated with the cross-wise direction agree with the result obtained for VIV-1dof;
- Jauvtis & Williamson point out $m^* \approx 6$ as a critical value, above which the cylinder does not oscillate in the in-line direction.

Characteristic curves, $m^* = 8.1, \zeta = 0.0018$.

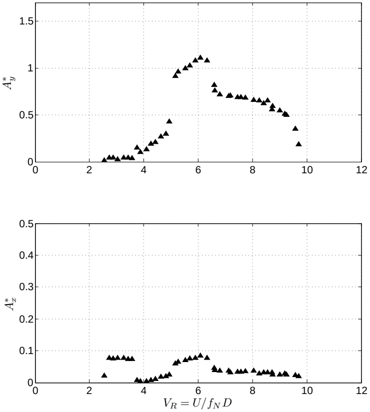

Extracted from Franzini et al (2012).

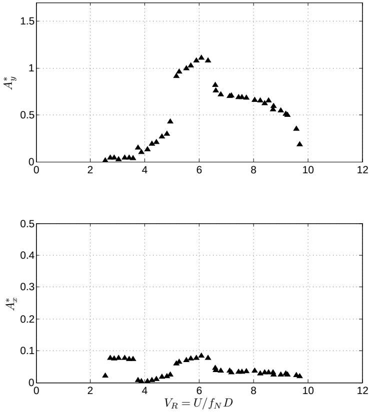

- Negligible in-line oscillations.

Extracted from Franzini et al (2012).

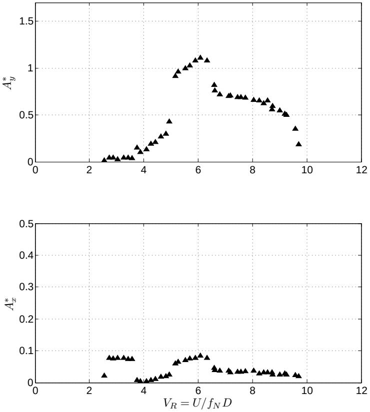

- Negligible in-line oscillations.
- In-line resonance $2 < V_R < 4$.

Extracted from Franzini et al (2012).

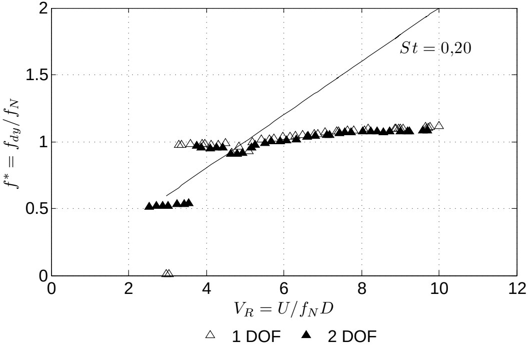

Extracted from Franzini et al (2012).

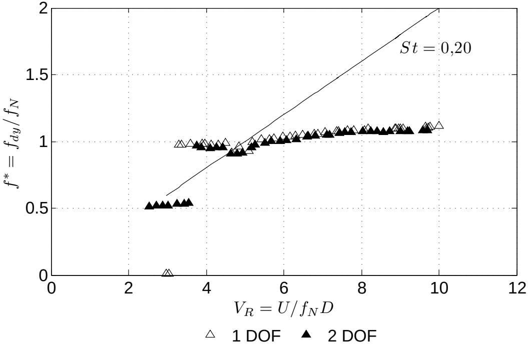

Extracted from Franzini et al (2012).

- Oscillation frequency tends to be constant and close to one for systems with high values of $m^*\zeta$.

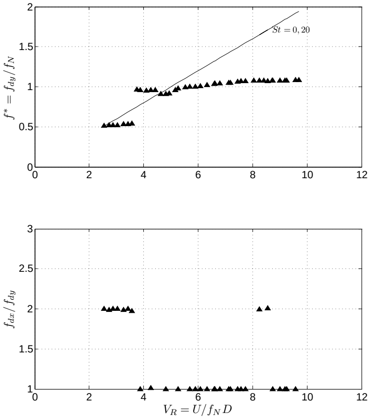

Extracted from Franzini et al (2012).

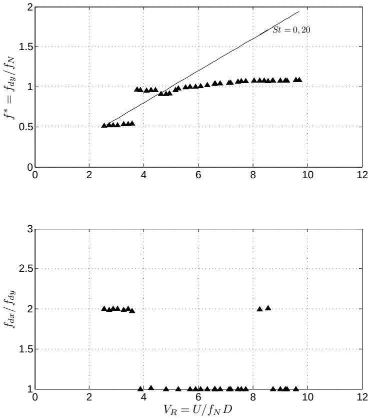

- In-line oscillations do not exhibit organized amplitude spectrum.

Extracted from Franzini et al (2012).

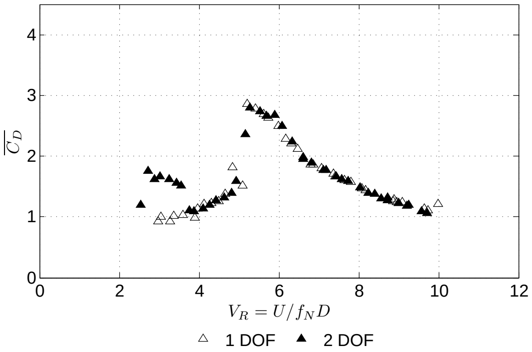

Extracted from Franzini et al (2012).

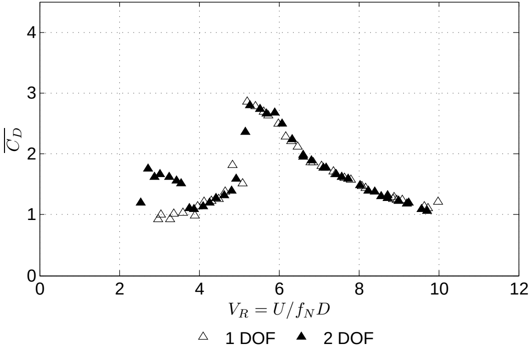

Extracted from Franzini et al (2012).

- The curve obtained from VIV-1dof match the one from VIV-2dof.

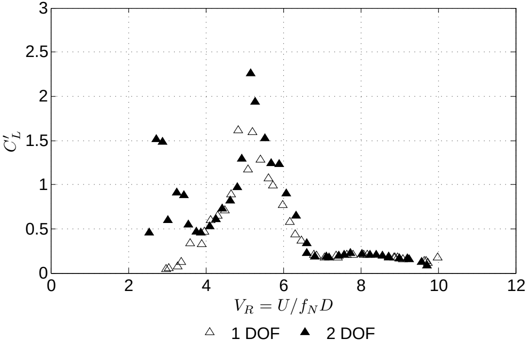

Extracted from Franzini et al (2012).

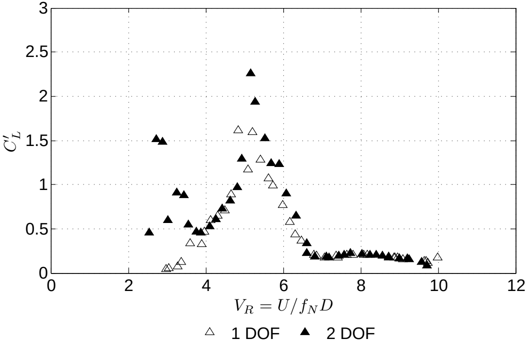

Extracted from Franzini et al (2012).

- The curve obtained from VIV-1dof match the one from VIV-2dof.

Programa de Pós-Graduação em Engenharia Civil
Escola Politécnica da Universidade de São Paulo

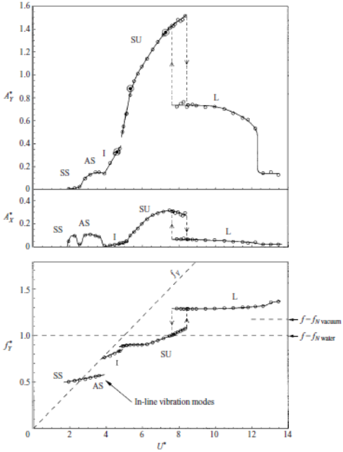

- $m^* = 2.6$.

Extracted from Jauvtis & Williamson (2004).

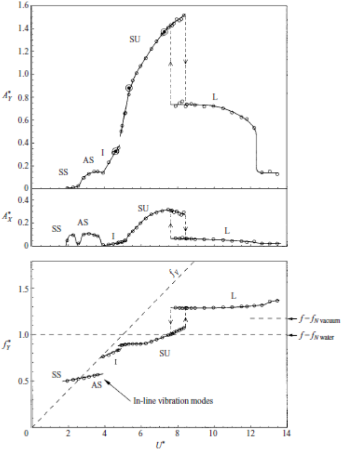

- $m^* = 2.6$.
- SS: Symmetric vortex-shedding;

Extracted from Jauvtis & Williamson (2004).

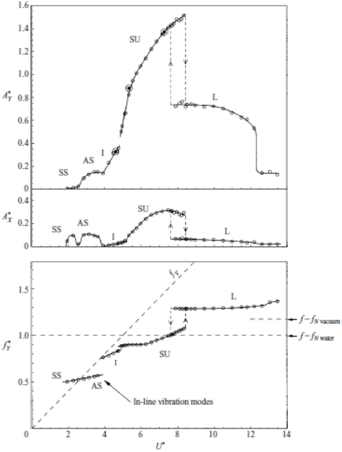

- $m^* = 2.6$.
- SS: Symmetric vortex-shedding;
- AS: Asymmetric vortex-shedding

Extracted from Jauvtis & Williamson (2004).

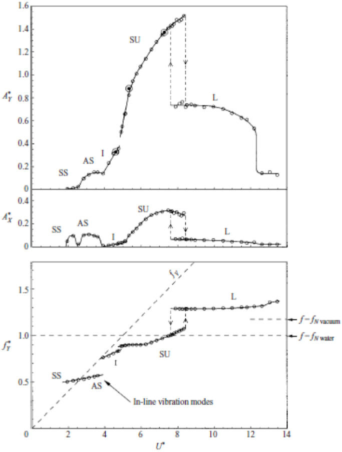

- $m^* = 2.6$.
- SS: Symmetric vortex-shedding;
- AS: Asymmetric vortex-shedding
- I: Initial branch

Extracted from Jauvtis & Williamson (2004).

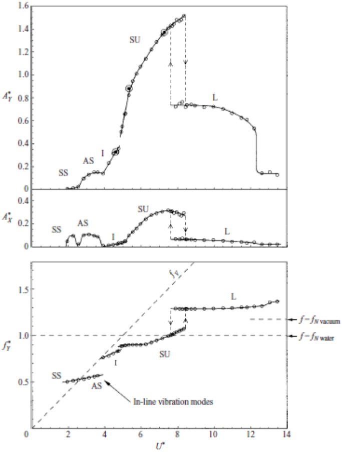

- $m^* = 2.6$.
- SS: Symmetric vortex-shedding;
- AS: Asymmetric vortex-shedding
- I: Initial branch
- SU: Super upper branch

Extracted from Jauvtis & Williamson (2004).

At the super-upper branch, two triplets of vortexes are shed at each oscillation cycle (2T pattern).

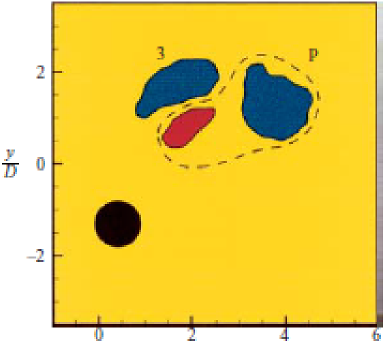

Extracted from Jauvtis & Williamson (2004).

- Oscillation amplitudes vary along the span;

Interesting aspects

- Oscillation amplitudes vary along the span;
- Multi-modal excitation can be observed;

- Oscillation amplitudes vary along the span;
- Multi-modal excitation can be observed;
- Possible existence of traveling waves;

- Oscillation amplitudes vary along the span;
- Multi-modal excitation can be observed;
- Possible existence of traveling waves;
- The dynamics of a flexible cylinder under VIV is intrinsically more complex than that observed on rigid and elastically mounted cylinder.

Programa de Pós-Graduação em Engenharia Civil
Escola Politécnica da Universidade de São Paulo

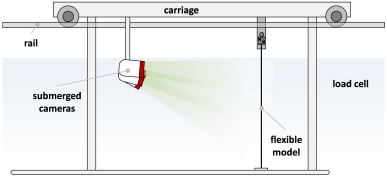

(a) Sketch of the side view.

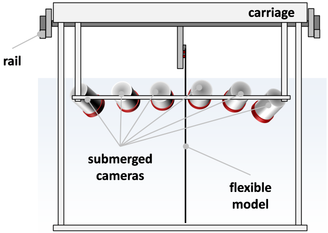

(b) Sketch of the back view.

Extracted from Franzini et al (2016).

Characteristic oscillation amplitude at $z/L_0 = 0.22$.

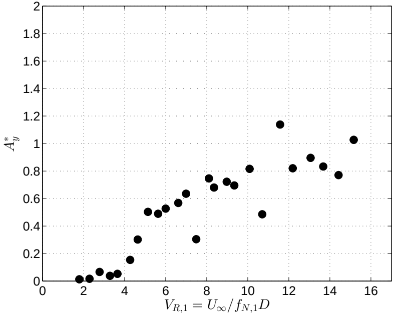

Extracted from Franzini et al (2016).

Characteristic oscillation amplitude at $z/L_0 = 0.22$.

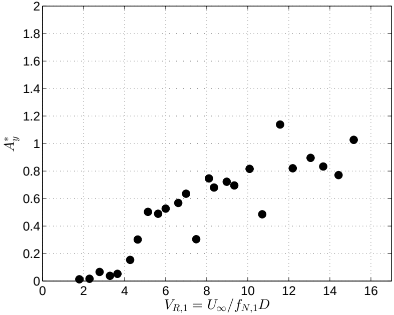

- No similarity with respect to the case in which the rigid cylinder is elastically supported is found.

Extracted from Franzini et al (2016).

Amplitude spectrum for a point at $z/L_0 = 0.22$.

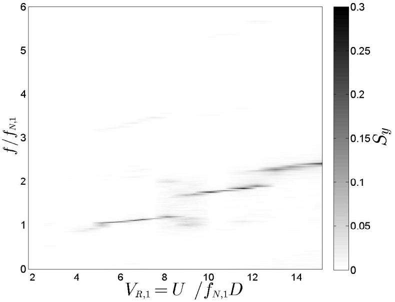

Extracted from Franzini et al (2016).

Amplitude spectrum for a point at $z/L_0 = 0.22$.

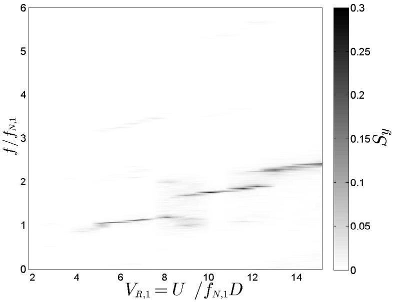

- Indicative of lock-in with different modes. (Free-decay tests allowed identifying that $f_{N,2} \approx 2f_{N,1}$ e $f_{N,3} \approx 3f_{N,1}$.

Extracted from Franzini et al (2016).

Time-history obtained at $z/L_0 = 0.43$.

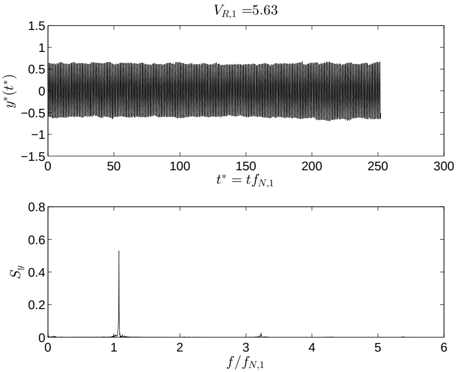

Extracted from Franzini et al (2018).

Time-history obtained at $z/L_0 = 0.43$.

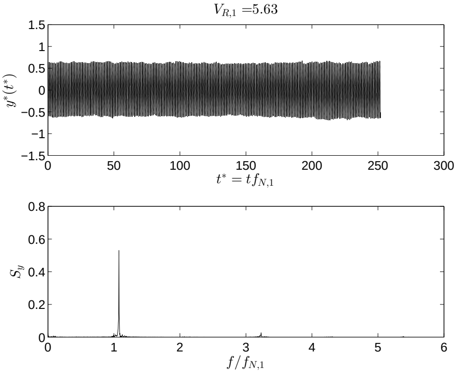

- Time-history practically free from amplitude modulation.

Extracted from Franzini et al (2018).

Time-history obtained at $z/L_0 = 0.43$.

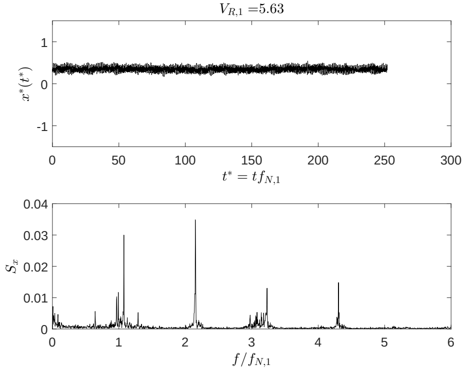

Extracted from Franzini et al (2018).

Time-history obtained at $z/L_0 = 0.43$.

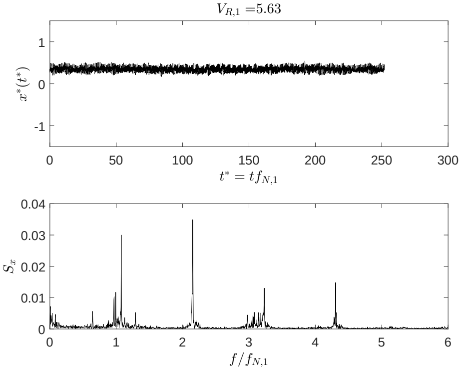

- Time-history practically from from amplitude modulation, but with a rich spectral content.

Extracted from Franzini et al (2018).

Amplitude spectra - Cross-wise direction.

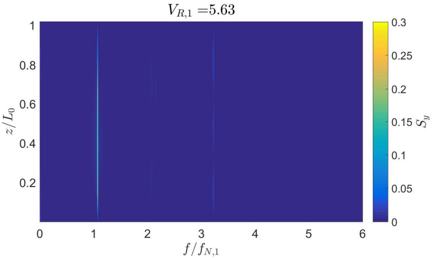

Extracted from Franzini et al (2018).

Amplitude spectra - Cross-wise direction.

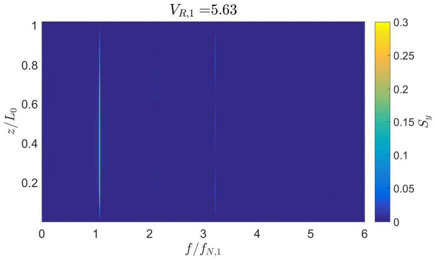

Extracted from Franzini et al (2018).

- Important responses on the odd modes.

Amplitude spectra - In-line direction

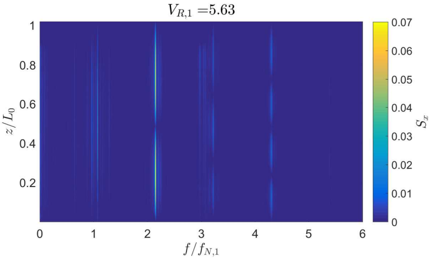

Extracted from Franzini et al (2018).

Amplitude spectra - In-line direction

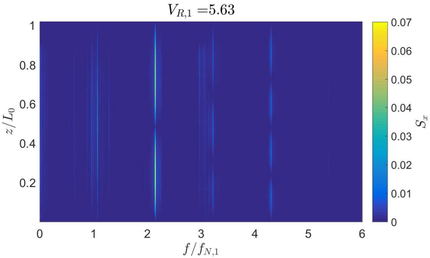

Extracted from Franzini et al (2018).

- Multimodal response, with predominance of the even modes.

Besides experiments in laboratory/field, VIV can be investigated using other two approaches, complementary to the experimental one.

- Computational Fluid Dynamics (CFD): Discretization of the domain for the solution of the Navier-Stokes equations → Turbulence modeling may be complex; high computational cost.

Besides experiments in laboratory/field, VIV can be investigated using other two approaches, complementary to the experimental one.

- Computational Fluid Dynamics (CFD): Discretization of the domain for the solution of the Navier-Stokes equations → Turbulence modeling may be complex; high computational cost.
- Wake-oscillator Models: Reduced-order models → We use non-linear equations for representing the fluid-structure interaction. These equations are coupled to the structural oscillators by means of empirically calibrated coefficients. This is the focus of the present notes.

Besides experiments in laboratory/field, VIV can be investigated using other two approaches, complementary to the experimental one.

- Computational Fluid Dynamics (CFD): Discretization of the domain for the solution of the Navier-Stokes equations $\rightarrow$ Turbulence modeling may be complex; high computational cost.
- Wake-oscillator Models: Reduced-order models $\rightarrow$ We use non-linear equations for representing the fluid-structure interaction. These equations are coupled to the structural oscillators by means of empirically calibrated coefficients. This is the focus of the present notes.
- Wake-oscillator models have been employed in VIV studies in the last decades (see, for example, Hartlen & Curie (1970), Iwan & Blevins (1974) and Parra & Aranha (1996));

Besides experiments in laboratory/field, VIV can be investigated using other two approaches, complementary to the experimental one.

- Computational Fluid Dynamics (CFD): Discretization of the domain for the solution of the Navier-Stokes equations $\rightarrow$ Turbulence modeling may be complex; high computational cost.
- Wake-oscillator Models: Reduced-order models $\rightarrow$ We use non-linear equations for representing the fluid-structure interaction. These equations are coupled to the structural oscillators by means of empirically calibrated coefficients. This is the focus of the present notes.
- Wake-oscillator models have been employed in VIV studies in the last decades (see, for example, Hartlen & Curie (1970), Iwan & Blevins (1974) and Parra & Aranha (1996));
- Focus of this class: Discussions of the models proposed in Facchinetti et al (2004) and in Ogink & Metrikine (2010).

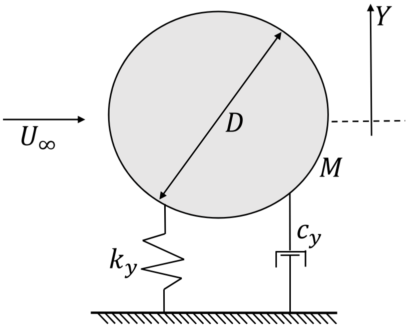

Extracted from Franzini (2019).

- Firstly, we consider Eq. 1.

$$\frac{d^2 q_y}{dt^2} + \epsilon_y \omega_f (q_y^2 - 1) \frac{dq_y}{dt} + \omega_s^2 q_y = 0 \tag{1}$$

- It can be shown that $q_y(t)$ oscillates with frequency ω_s and with steady-state amplitude $\hat{q}_y = 2$;
- In the problem of flow around a fixed cylinder: $C_L(t) = \hat{C}_L^0 \sin \omega_s t$;
- In a phenomenological way, we write the $C_L(t)$ as a function of $q_y(t)$ as $C_L(t) = \frac{\hat{C}_L^0}{\hat{q}_y} q_y(t)$.
- For modeling the effects of the cylinder oscillation onto the wake, Facchinetti et al. (2004) proposed to include a forcing term on the RHS of Eq. 1. After some systematic studies, they concluded that this term must be proportional to the cylinder acceleration $\frac{d^2 Y}{dt^2}$.

- Structural oscillator (hydrodynamic force F_y is decomposed onto two terms, one associated with potential flow - added mass effect - and a second one that accounts the viscous effects). Within this framework, the hydro-elastic system is governed by:

$$M\frac{d^2Y}{dt^2} + c_y\frac{dY}{dt} + k_y Y = F_{v,y} + F_p = \frac{1}{2}\rho U_\infty^2 DLC_{y,v} - m_a^{pot}\frac{d^2Y}{dt^2} \tag{2}$$

$$\frac{d^2q_y}{dt^2} + \epsilon_y\omega_f(q_y^2 - 1)\frac{dq_y}{dt} + \omega_f^2 q_y = \frac{A_y}{D}\frac{d^2Y}{dt^2} \tag{3}$$

- We write the mathematical model in the dimensionless form. For this, consider

$$\omega_{n,y} = 2\pi f_{n,y} = \sqrt{\frac{k_y}{M + m_a^{pot}}}, \quad \zeta_y = \frac{c_y}{2(M + m_a^{pot})\omega_{n,y}}, \; U_r = \frac{U_\infty}{f_{n,y}D}$$

$$y = \frac{Y}{D}, \quad \tau = \omega_{n,y}t, \quad \frac{d(\,)}{dt} = \omega_{n,y}(\dot{\,}), \; m^* = 4\frac{M}{\rho\pi D^2 L}, \quad C_a^{pot} = 4\frac{m_a^{pot}}{\rho\pi D^2 L} \tag{4}$$

- In these notes, U_r and V_R are the same quantity.

- Using $\dot{( )} = \frac{d( )}{d\tau}$, the dimensionless mathematical model reads

$$\ddot{y} + 2\zeta_y \dot{y} + y = \frac{1}{2\pi^3} \frac{U_r^2}{(m^* + C_a^{pot})} C_{y,v} \tag{5}$$

$$\ddot{q}_y + \epsilon_y St U_r (q_y^2 - 1)\dot{q}_y + (St U_r)^2 q_y = A_y \ddot{y} \tag{6}$$

- Now, we discuss how to obtain $C_{y,v}$. For this, consider the following figure

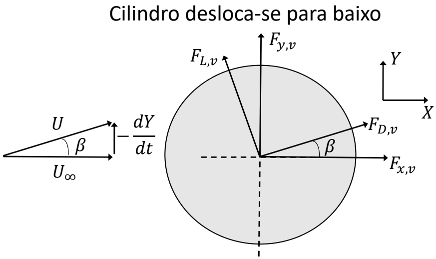

Extracted from Franzini (2019).

- In the model proposed by Facchinetti et al (2004) (and, some years latter, readdressed in Ogink & Metrikine (2010)), the viscous forces are obtained considering the relative velocity between the cylinder and the fluid U and the force coefficients obtained in the flow around a fixed cylinder;
- From the above figure, we have:

$$F_{v,y} = \frac{1}{2}\rho U_\infty^2 DLC_{y,v} = F_{L,v}\cos\beta + F_{D,v}\sin\beta \tag{7}$$

$$F_{D,v} = \frac{1}{2}\rho U^2 DLC_{D,v} \tag{8}$$

$$F_{L,v} = \frac{1}{2}\rho U^2 DLC_{L,v} \tag{9}$$

$$U = \sqrt{U_\infty^2 + \left(\frac{dY}{dt}\right)^2} = U_\infty\sqrt{1 + \left(\frac{2\pi\dot{y}}{U_r}\right)^2} \tag{10}$$

$$\sin\beta = \frac{-\frac{dY}{dt}}{U} = -\frac{D\omega_n\dot{y}}{U_\infty\sqrt{1 + \left(\frac{D\omega_n}{U_\infty}\dot{y}\right)^2}} = -\frac{2\pi\dot{y}}{U_r\sqrt{1 + \left(\frac{2\pi\dot{y}}{U_r}\right)^2}} \tag{11}$$

$$\cos\beta = \frac{U_\infty}{U} = \frac{1}{\sqrt{1 + \left(\frac{2\pi\dot{y}}{U_r}\right)^2}} \tag{12}$$

- Hence, we conclude that

$$C_{y,v} = \left(\frac{U}{U_\infty}\right)^2 (C_{L,v}\cos\beta + C_{D,v}\sin\beta) =$$

$$\left(C_{L,v}\frac{1}{\sqrt{1+\left(\frac{2\pi\dot{y}}{U_r}\right)^2}} - \frac{C_{D,v}}{U_r}\frac{2\pi\dot{y}}{\sqrt{1+\left(\frac{2\pi\dot{y}}{U_r}\right)^2}}\right)\left(1+\left(\frac{2\pi\dot{y}}{U_r}\right)^2\right) \tag{13}$$

- In a more compact form:

$$C_{y,v} = \left(C_{L,v} - \frac{C_{D,v}}{U_r}2\pi\dot{y}\right)\sqrt{1+\left(\frac{2\pi\dot{y}}{U_r}\right)^2} \tag{14}$$

- From the force coefficients associated with the flow around a fixed cylinder, $C_{D,v} = \bar{C}_D^0$ ("classical" mean drag coefficient) and

$$C_{L,v} = \frac{q_y}{\hat{q}_y}\hat{C}_L^0 \tag{15}$$

- The final version of the mathematical model is

$$\ddot{y} + 2\zeta_y \dot{y} + y = \frac{1}{2\pi^3} \frac{U_r^2}{(m^* + C_a^{pot})} \left[\left(\frac{q_y}{\hat{q}_y} \hat{C}_L^0 - \frac{C_{D,v} 2\pi \dot{y}}{U_r} \right) \sqrt{1 + \left(\frac{2\pi \dot{y}}{U_r} \right)^2} \right] \tag{16}$$

$$\ddot{q}_y + \epsilon_y St U_r (q_y^2 - 1)\dot{q}_y + (St U_r)^2 q_y = A_y \ddot{y} \tag{17}$$

- A_y and ϵ_y are coefficients that must be empirically calibrated;
- In Ogink & Metrikine (2010), the authors obtain another dimensionless mathematical model because they adopted as dimensionless time $\tau = tU_\infty / D$.

- Assumed hypothesis: The cylinder velocity $\frac{dY}{dt}$ is much smaller than the free-stream velocity U_∞. Mathematically, the authors assumed that

$$\frac{2\pi}{U_r}\dot{y} << 1 \tag{18}$$

- Using the above hypothesis, the dimensionless mathematical model developed in Facchinetti et al (2004) reads:

$$\ddot{y} + \left(2\zeta_y + \frac{C_{D,v}U_r}{\pi^2(m^* + C_a^{pot})}\right)\dot{y} + y = \frac{1}{2\pi^3}\frac{U_r^2}{(m^* + C_a^{pot})}\frac{\hat{C}_L^0}{\hat{q}_y}q_y \tag{19}$$

$$\ddot{q}_y + \epsilon_y StU_r(q_y^2 - 1)\dot{q}_y + (StU_r)^2 q_y = A_y\ddot{y} \tag{20}$$

- In Facchinetti et al (2004), the dimensionless mathematical model is different due to the chosen dimensionless time $\tau = tU_\infty/D$.

- Another difference between the wake-oscillator models proposed in Facchinetti et al (2004) and Ogink & Metrikine (2010) is the definition of the empirically calibrated parameters;
- Facchineeti et al (2004): A single pair of parameters (A_y, ϵ_y) for the whole range of reduced velocities;
- Ogink & Metrikine (2010): One pair of parameters (A_y, ϵ_y) for the upper branch and another one for the lower branch.

Facchinetti et al (2004)	
A_y	12
ϵ_y	0.30
$\hat{C}_L^0$	0.30
$C_{D,v} = \bar{C}_D^0$	2
St	0.20

Ogink & Metrikine (2010)		
	upper branch	lower branch
A_y	4	12
ϵ_y	0,05	0.7
$\hat{C}_L^0$	0.3842	
$C_{D,v} = \bar{C}_D^0$	1.1856	
St	0.1932	